# Identifying a new particle with jet substructures


Lim, Sung Hak

KAIST

ibS 기초과학연구원 Institute for Basic Science


Focus Workshop on Particle Physics and Cosmology, IBS-CTPU

Dec. 6. 2016


C. Han, D. Kim, M. Kim, K. Kong, **S. H. Lim** and M. Park, accepted by JHEP, [arXiv:1609.06205 [hep-ph]].

# Mass spectrum of Higgs sector in MSSM

- Many theories beyond the Standard model (SUSY, composite Higgs...) could have extended Higgs sector with particles having masses more than $\mathcal{O}(1)$ TeV to make model compatible with the current observation about the Higgs boson.
  - Example: heavy Higgs boson in MSSM
- mass eigenstates ( $\tan\beta = v_u/v_d$ )

$$m^2_{A^0} = \frac{2b}{\sin 2\beta} \quad (1)$$

$$m^2_{H^\pm} = m^2_{A^0} + m^2_W \quad (2)$$

$$m^2_{h^0,H^0} = \frac{1}{2}\left(m^2_{A^0} + m^2_Z \mp \sqrt{(m^2_{A^0} - m^2_Z)^2 + 4m^2_Z m^2_{A^0} sin^2 2\beta}\right) \quad (3)$$

- In a limit $m_{A^0} \gg m_Z$ ( decoupling limit ),

$$m_Z \sim m_{h^0} \ll m_{H^0} \sim m_{H^\pm} \sim m_{A^0} \quad (4)$$

- $h^0$ behaves like the Higgs boson in the Standard model, while other heavy scaler lives in higher energy scale.
- One interesting channel for identifying heavy Higgs bosons is $ZZ$ channel.

# Characteristics of $X \to ZZ$ channel

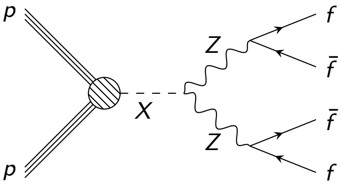

# Characteristics of $X \to ZZ$ channel

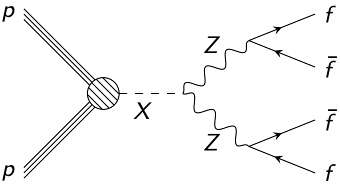


- Good: this channel is fully capable of determining spin and CP nature of $X$.

# Characteristics of $X \to ZZ$ channel

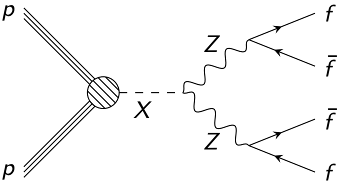


- Good: this channel is fully capable of determining spin and CP nature of $X$.
  - $\gamma\gamma$: polarization-blind, we cannot fully determine spin and $CP$ of $X$.
  - $ZZ$: we can get additional polarization information of $Z$ boson from differential distribution of Fermions.

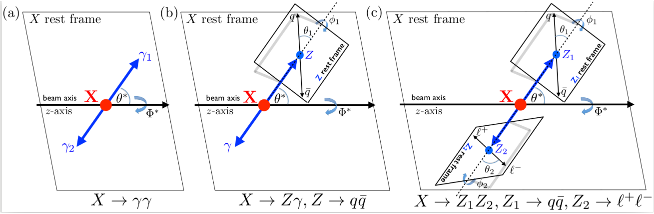

## Characteristics of $X \to ZZ$ channel

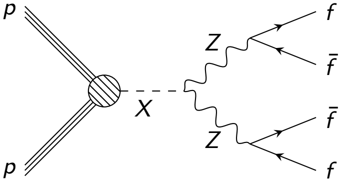


- Good: this channel is fully capable of determining spin and CP nature of $X$.
- Problem: (For heavy $X$, $m_X \gg m_Z$) $Z$ boson is boosted, and two Fermions (especially quarks) are often too close and identified as a single large cluster.

# Characteristics of $X \rightarrow ZZ$ channel

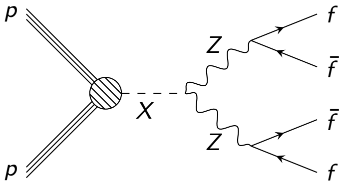


- Good: this channel is fully capable of determining spin and CP nature of $X$.
- Problem: (For heavy $X$, $m_X \gg m_Z$) $Z$ boson is boosted, and two Fermions (especially quarks) are often too close and identified as a single large cluster.
  - In order to use full potential of $ZZ$ channel, We should resolve the cluster.
  - We will see that the jet substructure technique can resolve the cluster and effectively select statistically sensitive kinematic region for discriminating spin and CP of $X$.

# Characteristics of $X \to ZZ$ channel

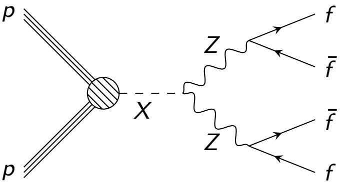


- Good: this channel is fully capable of determining spin and CP nature of $X$.
- Problem: (For heavy $X$, $m_X \gg m_Z$) $Z$ boson is boosted, and two Fermions (especially quarks) are often too close and identified as a single large cluster.
    - In order to use full potential of $ZZ$ channel, We should resolve the cluster.
    - We will see that the jet substructure technique can resolve the cluster and effectively select statistically sensitive kinematic region for discriminating spin and CP of $X$.
- Example: mass-drop tagger
  ( J. M. Butterworth, A. R. Davison, M. Rubin and G. P. Salam, arXiv:0802.2470)

# Identifying boosted $Z \to q\bar{q}$ with merged jet

- We can identify momenta of two prong subjets by the mass-drop tagger.

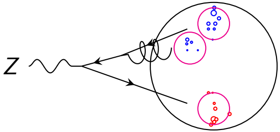


- Merged jet identification: Cambridge-Aachen algorithm with large radius
- Jet substructure for identifying $q\bar{q}$
  - mass-drop and filtering: look for subclusters with lighter masses

$$m_{j_1} < \mu m_j \tag{5}$$

and symmetric $p_T$

$$\frac{\min(p^2_{T,j_1}, p^2_{T,j_2})}{m_j^2}(\Delta R_{j_1 j_2})^2 > y_{\rm cut} \tag{6}$$

- This subjet momenta can be used for identifying CP state of $S$!

## boosted $Z$ boson to leptons vs quarks

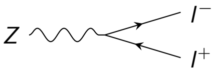


vs

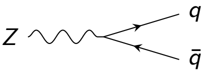


- advantages
- disadvantages

# boosted $Z$ boson to leptons vs quarks


- advantages
  - more events!

$$
\begin{aligned}
BR(Z \to e^+e^-) &= 3.363\% \\
BR(Z \to \mu^+\mu^-) &= 3.366\% \\
BR(Z \to \text{invisible}) &= 20.00\% \\
BR(Z \to \text{hadrons}) &= 69.91\%
\end{aligned}
$$

- disadvantages

# boosted $Z$ boson to leptons vs quarks

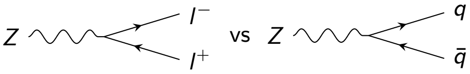


- advantages
  - more events!

$$
\begin{aligned}
BR(Z \to e^+e^-) &= 3.363\% \\
BR(Z \to \mu^+\mu^-) &= 3.366\% \\
BR(Z \to \text{invisible}) &= 20.00\% \\
BR(Z \to \text{hadrons}) &= 69.91\%
\end{aligned}
$$

- disadvantages
  - hard to resolve two close quarks.

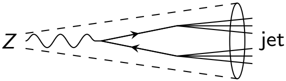

# boosted $Z$ boson to leptons vs quarks

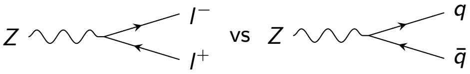


- advantages
  - more events!

$$
\begin{aligned}
BR(Z \to e^+e^-) &= 3.363\% \\
BR(Z \to \mu^+\mu^-) &= 3.366\% \\
BR(Z \to \text{invisible}) &= 20.00\% \\
BR(Z \to \text{hadrons}) &= 69.91\%
\end{aligned}
$$

- disadvantages
  - hard to resolve two close quarks.

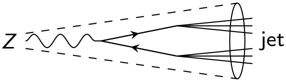


  - contamination from nearby QCD activity
    - underlying events
    - final state radiations
    - pile-ups

# boosted $Z$ boson to leptons vs quarks

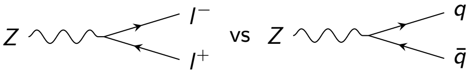


- advantages
  - more events!

$$
\begin{aligned}
BR(Z \to e^+e^-) &= 3.363\% \\
BR(Z \to \mu^+\mu^-) &= 3.366\% \\
BR(Z \to \text{invisible}) &= 20.00\% \\
BR(Z \to \text{hadrons}) &= 69.91\%
\end{aligned}
$$

- disadvantages
  - hard to resolve two close quarks.

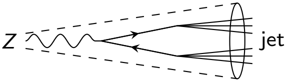


  - contamination from nearby QCD activity
    - underlying events
    - final state radiations
    - pile-ups
    - Many background events..

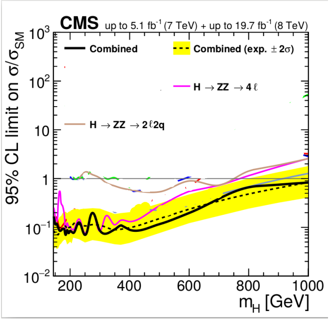


- $ZZ \to 2\ell 2q$ having same sensitivity level to the $ZZ \to 4\ell$ in high mass resonance searches.
- Q: is obtained subjet information really reliable for identifying quantum state of $H$? - YES!

# Benchmark point

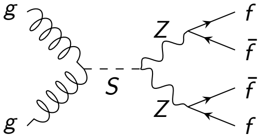


We particularly considered scalar resonances in CP eigenstate.

# Benchmark point

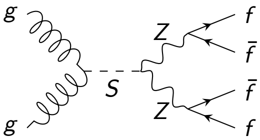


We particularly considered scalar resonances in CP eigenstate.

$$\mathcal{L}_{0^{++}} = \frac{c_{gg}}{\Lambda} S G_{\mu\nu} G^{\mu\nu} + \frac{c_{ZZ}}{\Lambda} S Z_{\mu\nu} Z^{\mu\nu}$$

# Benchmark point

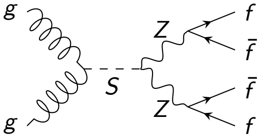


We particularly considered scalar resonances in CP eigenstate.

$$\mathcal{L}_{0^{++}} = \frac{c_{gg}}{\Lambda} S G_{\mu\nu} G^{\mu\nu} + \frac{c_{ZZ}}{\Lambda} S Z_{\mu\nu} Z^{\mu\nu}$$
$$\mathcal{L}_{0^{-+}} = \frac{c_{gg}}{\Lambda} S G_{\mu\nu} \tilde{G}^{\mu\nu} + \frac{c_{ZZ}}{\Lambda} S Z_{\mu\nu} \tilde{Z}^{\mu\nu}$$

# Benchmark point

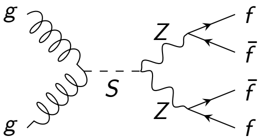


| benchmark points | $r_M$ | $\Delta R \gtrsim$ |
|---|---|---|

We particularly considered scalar resonances in CP eigenstate.

$$\mathcal{L}_{0^{++}} = \frac{c_{gg}}{\Lambda} S G_{\mu\nu} G^{\mu\nu} + \frac{c_{ZZ}}{\Lambda} S Z_{\mu\nu} Z^{\mu\nu}$$

$$\mathcal{L}_{0^{-+}} = \frac{c_{gg}}{\Lambda} S G_{\mu\nu} \tilde{G}^{\mu\nu} + \frac{c_{ZZ}}{\Lambda} S Z_{\mu\nu} \tilde{Z}^{\mu\nu}$$

# Benchmark point

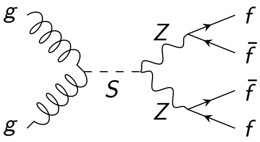


| benchmark points | $r_M$ | $\Delta R \gtrsim$ |
|---|---|---|
| $m_S = 750\,\mathrm{GeV}$ | 4.1 | 0.5 |

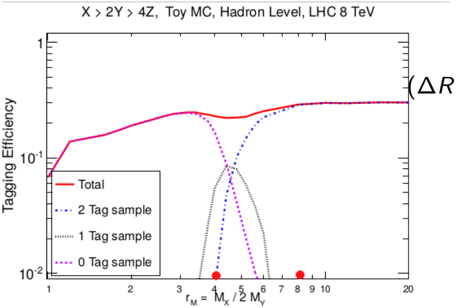


M. Gouzevitch, et al., arXiv:1303.6636

$$r_M = \frac{m_S}{2m_Z}$$

$$(\Delta R) = \sqrt{(\Delta\eta)^2 + (\Delta\phi)^2} \gtrsim \frac{4m_Z}{\sqrt{m_S^2 - 4m_Z^2}}$$

# Benchmark point

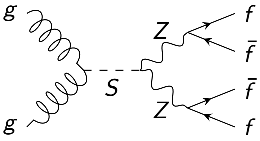


| benchmark points | $r_M$ | $\Delta R \gtrsim$ |
|---|---|---|
| $m_S = 750\,\mathrm{GeV}$ | 4.1 | 0.5 |
| $m_S = 1500\,\mathrm{GeV}$ | 8.2 | 0.25 |

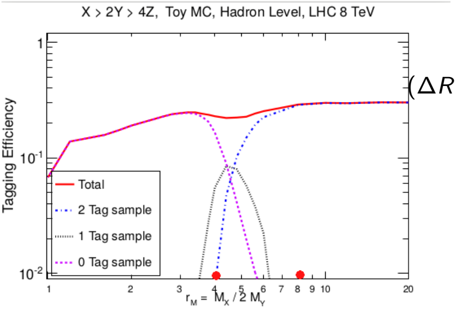


M. Gouzevitch, et al., arXiv:1303.6636

$$r_M = \frac{m_S}{2m_Z}$$

$$(\Delta R) = \sqrt{(\Delta\eta)^2 + (\Delta\phi)^2} \gtrsim \frac{4m_Z}{\sqrt{m_S^2 - 4m_Z^2}}$$

# Benchmark point

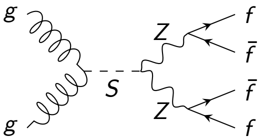


| benchmark points | $r_M$ | $\Delta R \gtrsim$ |
|---|---|---|
| $m_S = 750\,\mathrm{GeV}$ | 4.1 | 0.5 |
| $m_S = 1500\,\mathrm{GeV}$ | 8.2 | 0.25 |

We particularly considered scalar resonances in CP eigenstate.

$$\mathcal{L}_{0^{++}} = \frac{c_{gg}}{\Lambda} S G_{\mu\nu} G^{\mu\nu} + \frac{c_{ZZ}}{\Lambda} S Z_{\mu\nu} Z^{\mu\nu}$$

$$\mathcal{L}_{0^{-+}} = \frac{c_{gg}}{\Lambda} S G_{\mu\nu} \tilde{G}^{\mu\nu} + \frac{c_{ZZ}}{\Lambda} S Z_{\mu\nu} \tilde{Z}^{\mu\nu}$$

We performed statistical analysis with Monte Carlo simulated event together with detector simulations.

# Quantum interference and angular correlations

- In order to identify spin and CP of $S$, angular correlation between resonances are the key signatures.

# Quantum interference and angular correlations

- In order to identify spin and CP of $S$, angular correlation between resonances are the key signatures.
- In particular, angular correlation between two $Z$ boson system is especially useful for identifying CP of $S$, because $\mathcal{L}_{0^{\pm+}}$ produce two $Z$ boson in entangled helicity eigenstate ($\epsilon_{\pm}$).

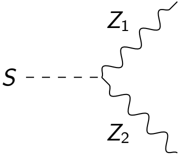


$$\propto \begin{cases} \epsilon_+^{*\mu}(Z_1)\epsilon_+^{*\nu}(Z_2) + \epsilon_-^{*\mu}(Z_1)\epsilon_-^{*\nu}(Z_2) & S \text{ in } \mathcal{L}_{0^{++}} \\ \epsilon_+^{*\mu}(Z_1)\epsilon_+^{*\nu}(Z_2) - \epsilon_-^{*\mu}(Z_1)\epsilon_-^{*\nu}(Z_2) & S \text{ in } \mathcal{L}_{0^{-+}} \end{cases}$$

($m_X \gg m_Z$ is assumed)

# Quantum interference and angular correlations

- In order to identify spin and CP of $S$, angular correlation between resonances are the key signatures.
- In particular, angular correlation between two $Z$ boson system is especially useful for identifying CP of $S$, because $\mathcal{L}_{0\pm+}$ produce two $Z$ boson in entangled helicity eigenstate ($\epsilon_\pm$).

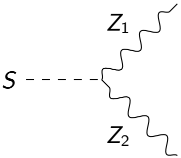


$$\propto \begin{cases} \epsilon_+^{*\mu}(Z_1)\epsilon_+^{*\nu}(Z_2) + \epsilon_-^{*\mu}(Z_1)\epsilon_-^{*\nu}(Z_2) & S \text{ in } \mathcal{L}_{0++} \\ \epsilon_+^{*\mu}(Z_1)\epsilon_+^{*\nu}(Z_2) - \epsilon_-^{*\mu}(Z_1)\epsilon_-^{*\nu}(Z_2) & S \text{ in } \mathcal{L}_{0-+} \end{cases}$$

- Angular correlation arise from interference between helicity eigenstates.

# Quantum interference and angular correlations

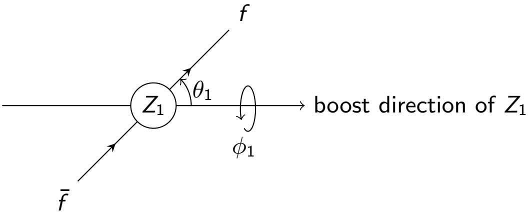


- Interference term leaves an azimuthal phase factor so it can be captured by angular correlations.

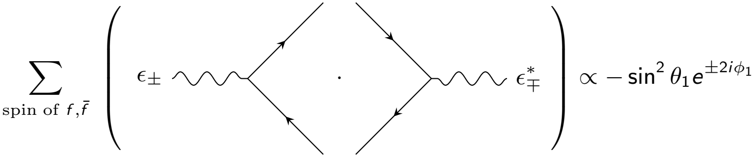


- Interference term is maximized when $f\bar{f}$ are emitted to transverse direction. This is consequence of the Stern-Gerlach experiment, $[S_z, S_x] \neq 0$.

# Quantum interference and angular correlations

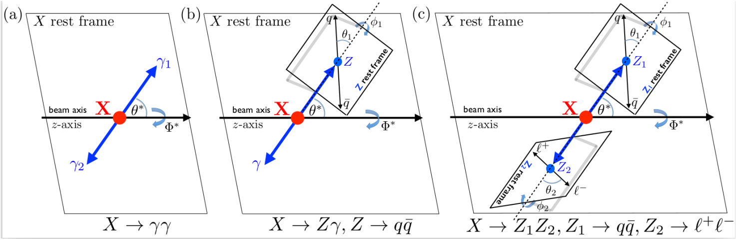


- As a result $\phi = \phi_1 - \phi_2$, which is the angle between two $Z$ boson decay plane, can discriminate CP of $S$.

# Quantum interference and angular correlations

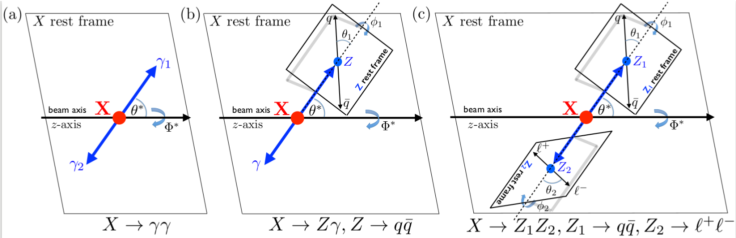


- As a result $\phi = \phi_1 - \phi_2$, which is the angle between two $Z$ boson decay plane, can discriminate CP of $S$.

$$\sum_{\text{spin of } q,\bar{q},\ell^-,\ell^-} \left| \cdots \right|^2 \propto (1+\cos^2\theta_1)(1+\cos^2\theta_2) \pm \sin^2\theta_1 \sin^2\theta_2 \cos 2\phi$$

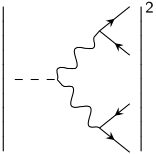

for $S$ in $\mathcal{L}_{0^{\pm+}}$, $m_S \gg m_Z$ .

# Quantum interference and angular correlations

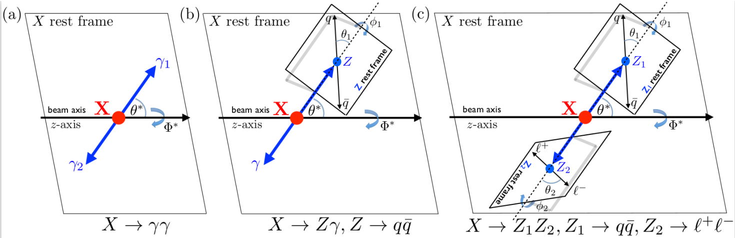


- As a result $\phi = \phi_1 - \phi_2$, which is the angle between two $Z$ boson decay plane, can discriminate CP of $S$.

$$\sum_{\text{spin of } q,\bar{q},\ell^-,\ell^-} \left| \quad \right|^2 \propto (1+\cos^2\theta_1)(1+\cos^2\theta_2) \pm \sin^2\theta_1 \sin^2\theta_2 \cos 2\phi$$

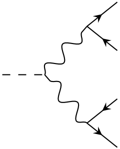

for $S$ in $\mathcal{L}_{0^{\pm+}}$, $\quad m_S \gg m_Z$ .

- Becase of sin factors, the sensitivity will depends how we choose Fermions.

# Relativistic Aberration and angular separation of $f\bar{f}$

When we try to capture two $q\bar{q}$ by a single merged jet, Fermions emitted transverse direction from the boost direction of $Z$ boson will be captured more than the longitudinal direction.

# Relativistic Aberration and angular separation of $f\bar{f}$

When we try to capture two $q\bar{q}$ by a single merged jet, Fermions emitted transverse direction from the boost direction of $Z$ boson will be captured more than the longitudinal direction.

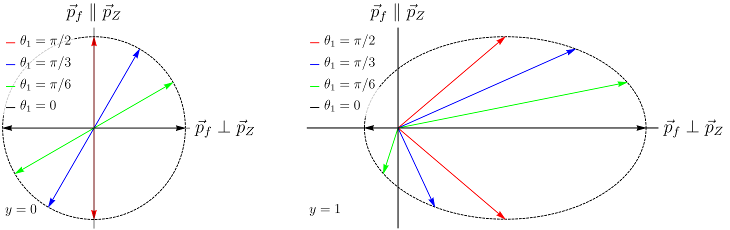


- For boosted object, phase space is beamed forward in a lab frame.

# Relativistic Aberration and angular separation of $f\bar{f}$

When we try to capture two $q\bar{q}$ by a single merged jet, Fermions emitted transverse direction from the boost direction of $Z$ boson will be captured more than the longitudinal direction.

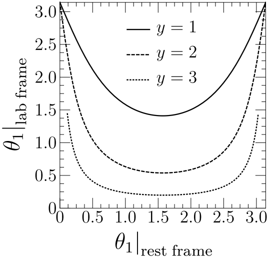


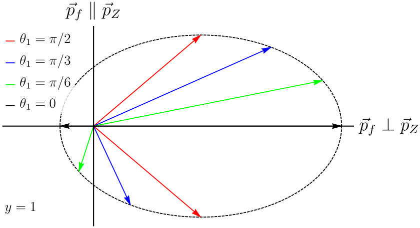


- For boosted object, phase space is beamed forward in a lab frame.
- For $Z \to f\bar{f}$, transverse direction is more collimated than the longitudinal direction.

# Relativistic Aberration and angular separation of $f\bar{f}$

When we try to capture two $q\bar{q}$ by a single merged jet, Fermions emitted transverse direction from the boost direction of $Z$ boson will be captured more than the longitudinal direction.

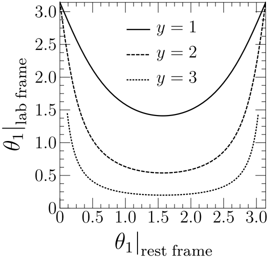


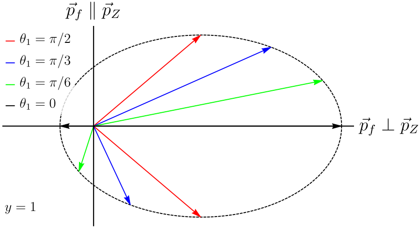


- For boosted object, phase space is beamed forward in a lab frame.
- For $Z \to f\bar{f}$, transverse direction is more collimated than the longitudinal direction.
- Because the interference term maximized in the transverse direction, using merged jet is still effective for analysing CP property of $S$.

# Distribution of $\phi$

- The key signature for identifying CP state of $S$ is angle $\phi$ between decay plane of $Z$ bosons.

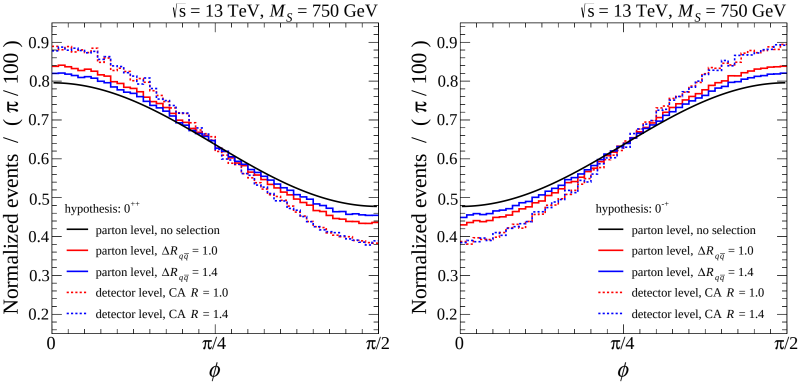


- Even we can still observe significant difference between $\phi$ distribution using subjet information!

# Distribution of $\phi$

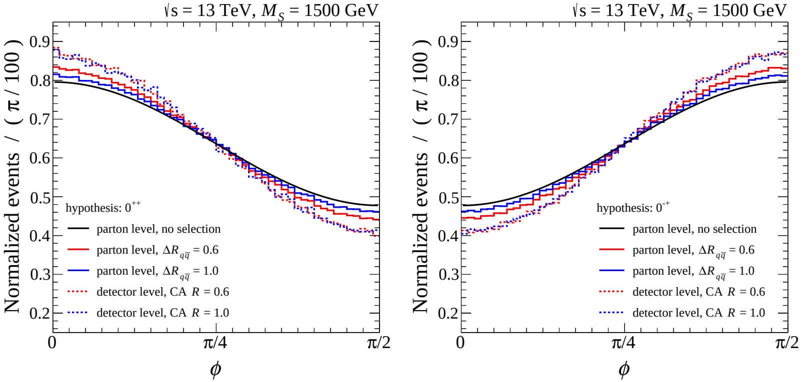


- Even we can still observe significant difference between $\phi$ distribution in highly boosted regime!

# Signal only analysis

In order to quantify the difference between CP even and CP odd scalar, we performed statistical analysis (matrix element method).

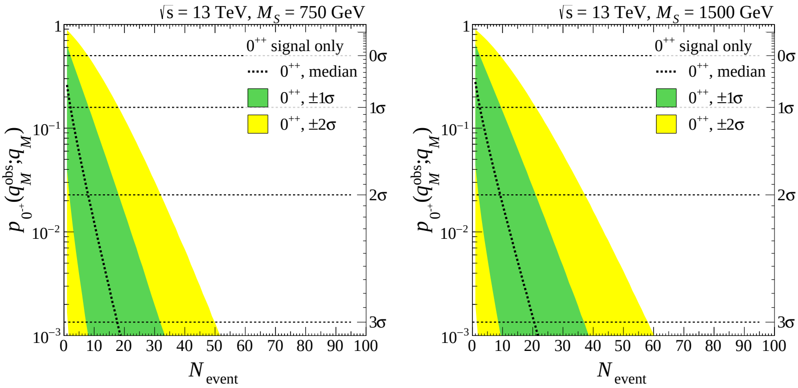


If we have $\sim 20$ events, we can distingush CP even and CP odd hypothesis!

# Analysis with background

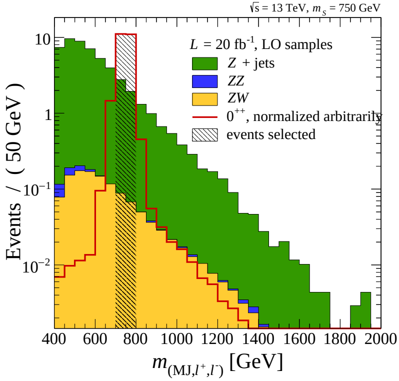


- QCD :
  $Z(\to \ell^- \ell^+) + \text{jets(fake } Z)$
- EW :
  $Z(\to \ell^- \ell^+) + V\ (\to q\bar{q})$

# Analysis with background

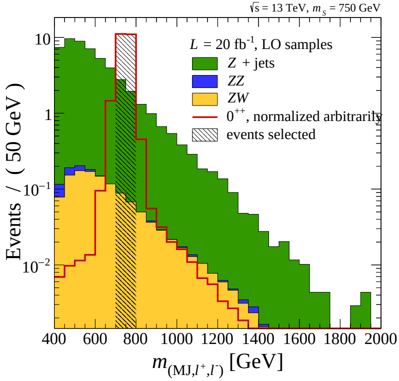


- QCD : $Z(\to \ell^- \ell^+) + \text{jets(fake } Z)$
- EW : $Z(\to \ell^- \ell^+) + V\ (\to q\bar{q})$
- $Z$+jets is dominant background because of large cross section.

# Analysis with background

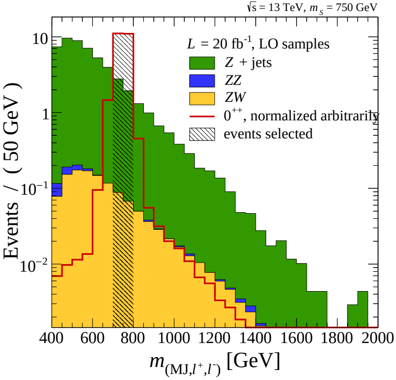


- QCD :
  $Z(\to \ell^- \ell^+) + \text{jets(fake } Z)$
- EW :
  $Z(\to \ell^- \ell^+) + V\ (\to q\bar{q})$
- $Z$+jets is dominant background because of large cross section.
- We just inject background to our statistical analysis.

# Analysis with background

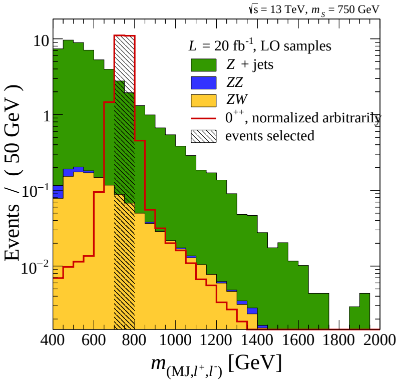


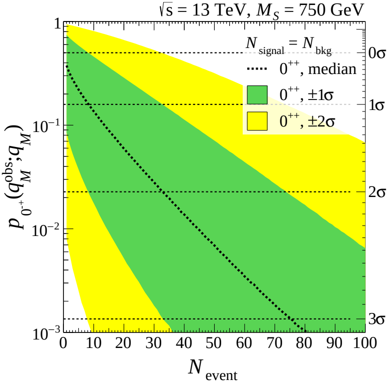

# Analysis with background

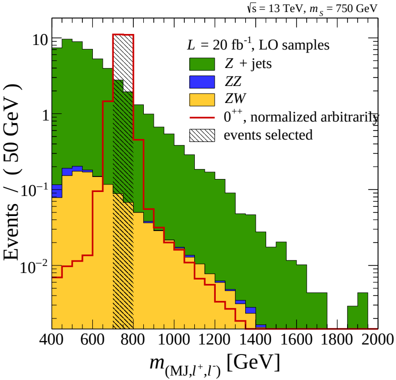


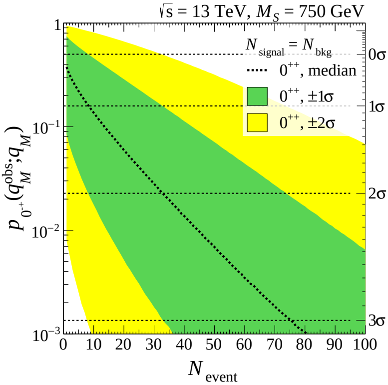


Jet substructure analysis is still effective even with background events.

# Conclusion

- Boosted object analysis is necessary in order to understand spin and CP nature of heavy intermediate resonance $S$ in $S \to ZZ$ channel.
- Merged jet analysis with jet substructure effectively select most sensitive region for identifying CP property of $S$.
- We can find out CP state of $S$ in $S \to ZZ \to q\bar{q}\ell^- \ell^-$ from subjet momenta with matrix element method.

# Backups

# Event selection criterion

| Cut flow | selection | 750 GeV | 1500 GeV |
|---|---|---|---|
| parton level | | 100.0 % | 100.0 % |
| object tagging | one merged jet, two $\ell$ | 61.0 % | 63.4 % |
| lepton $P_T$ | $P_T > 25$ GeV | 52.0 % | 58.8 % |
| $m_{(\ell^+,\,\ell^-)}$ | $[83, 99]$ GeV | 47.4 % | 53.5 % |
| $m_{\mathrm{MJ}}$ | $[75, 105]$ GeV | 20.6 % | 25.5 % |
| $y_{ZZ}$ | $\lvert y_{ZZ}\rvert < 0.15$ | 16.3 % | 21.3 % |
| $P_{T(\mathrm{MJ})}$ | $P_{T(\mathrm{MJ})} > 0.4\, m_{(\mathrm{MJ},\,\ell^+,\,\ell^-)}$ | 11.5 % | 14.7 % |
| $m_{(\mathrm{MJ},\,\ell^+,\,\ell^-)}$ | within $M_S \pm 50$ GeV | 10.4 % | - |
| | within $M_S \pm 100$ GeV | - | 13.4 % |

# Event selection criterion

| | BP1 ($M_S = 750$ GeV) | | | |
|---|---|---|---|---|
| cut flow | selection criterion | $\sigma_{Z+\text{jets}}$ | $\sigma_{ZZ}$ | $\sigma_{ZW}$ |
| parton level | $P_T$ of leading jet $\geq$ 150 GeV | 8.65 pb | 8.19 fb | 8.96 fb |
| object tagging | One merged jet, two $\ell$ | 44.11% | 55.30% | 55.83% |
| lepton $P_T$ | $P_T > 25$ GeV | 33.47% | 44.88% | 47.24% |
| $m_{(\ell^+, \ell^-)}$ | $[83, 99]$ GeV | 30.54% | 40.91% | 42.92% |
| $m_{\text{MJ}}$ | $[75, 105]$ GeV | 1.60% | 12.10% | 10.72% |
| $y_{ZZ}$ | $\|y_{ZZ}\| < 0.15$ | 0.72% | 11.06% | 9.83% |
| $P_{T(\text{MJ})}$ | $P_{T(\text{MJ})} > 0.4\, m_{(\text{MJ}, \ell^+, \ell^-)}$ | 0.48% | 7.22% | 5.29% |
| $m_{(\text{MJ}, \ell^+, \ell^-)}$ | within $M_S \pm 50$ GeV | 0.037% | 0.82% | 0.68% |
| Cross section ($\sigma$) | - | 3.16 fb | 0.0671 fb | 0.0609 fb |

# Matrix element methods

- We deployed a matrix element method in order to maximize discrimination power.
- Neyman-Pearson lemma says: likelihood ratio test is the most powerful test.
- At the parton level, we can find out the analytic form of probability from the theory as well as the likelihood functions for the hypothesis test. At the leading order, the probability density function is

$$f(\{p\}|0^{\pm}) = \frac{1}{N_{0^{\pm}}} \int dx_1 \int dx_2 f_g(x_1) f_g(x_2) \left|\mathcal{M}_{gg\to S\to q\bar{q}\ell^-\ell^+}(\{p\}|0^{\pm+})\right|^2$$

- Since $S$ is a scalar, we can factorize the matrix element in a narrow width limit.

$$f(\{p\}|0^{\pm}) = \frac{1}{N'_{0^{\pm}}} \int dx_1 \int dx_2 f_g(x_1) f_g(x_2) \left|\mathcal{M}_{gg\to S}(\{p\}|0^{\pm+})\right|^2 \cdot \left|\mathcal{M}_{S\to q\bar{q}\ell^-\ell^+}(\{p\}|0^{\pm+})\right|^2$$

# Matrix element methods

- The likelihood ratio can be simplified if we assume

$$\frac{1}{N'_{0^{\pm+}}} \int dx_1 \int dx_2 f_g(x_1) f_g(x_2) |\mathcal{M}_{gg \to S}(\{p\}|0^{\pm+})|^2 \tag{7}$$

are identical for $0^{++}$ and $0^{-+}$. The likelihood ratio can be written in terms of matrix element of the decay only.

$$\frac{f(\{p\}|0^{++})}{f(\{p\}|0^{-+})} = \frac{|\mathcal{M}_{S \to q\bar{q}\ell^-\ell^+}(\{p\}|0^{++})|^2}{|\mathcal{M}_{S \to q\bar{q}\ell^-\ell^+}(\{p\}|0^{-+})|^2} \tag{8}$$

- We further symmetrize momenta of quarks since $q$ and $\bar{q}$ are indistingushable at LHC. Then, we define a loglikelihood ratio

$$q_{\mathcal{M}} = \sum_i^N \ln \frac{|\mathcal{M}(\{p\}_i|0^{++})|^2_{sym}}{|\mathcal{M}(\{p\}_i|0^{-+})|^2_{sym}} \tag{9}$$

# Cambridge/Aachen Algorithm

Cambridge/Aachen Algorithm: a sequential clustering algorithm with a distance measure $(\Delta R)^2 = (\Delta\eta)^2 + (\Delta\phi)^2$

# Cambridge/Aachen Algorithm

Cambridge/Aachen Algorithm: a sequential clustering algorithm with a distance measure $(\Delta R)^2 = (\Delta\eta)^2 + (\Delta\phi)^2$

1. Check distances between objects.

# Cambridge/Aachen Algorithm

Cambridge/Aachen Algorithm: a sequential clustering algorithm with a distance measure $(\Delta R)^2 = (\Delta\eta)^2 + (\Delta\phi)^2$

1. Check distances between objects.
2. Choose a pair of object having smallest $\Delta R$.

# Cambridge/Aachen Algorithm

Cambridge/Aachen Algorithm: a sequential clustering algorithm with a distance measure $(\Delta R)^2 = (\Delta\eta)^2 + (\Delta\phi)^2$

1. Check distances between objects.
2. Choose a pair of object having smallest $\Delta R$.
3. If the two object are separated by $\Delta R$ smaller than the threshold distance $R$, then merge the two objects in a shortest distance by summing their momenta.

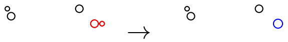

$\Delta R < R$

# Cambridge/Aachen Algorithm

Cambridge/Aachen Algorithm: a sequential clustering algorithm with a distance measure $(\Delta R)^2 = (\Delta\eta)^2 + (\Delta\phi)^2$

1. Check distances between objects.
2. Choose a pair of object having smallest $\Delta R$.
3. If the two object are separated by $\Delta R$ smaller than the threshold distance $R$, then merge the two objects in a shortest distance by summing their momenta.
4. Iterate above steps until every objects are separated by the threshold distance $R$.

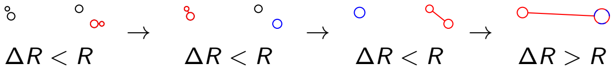

# Cambridge/Aachen Algorithm

Cambridge/Aachen Algorithm: a sequential clustering algorithm with a distance measure $(\Delta R)^2 = (\Delta\eta)^2 + (\Delta\phi)^2$

1. Check distances between objects.
2. Choose a pair of object having smallest $\Delta R$.
3. If the two object are separated by $\Delta R$ smaller than the threshold distance $R$, then merge the two objects in a shortest distance by summing their momenta.
4. Iterate above steps until every objects are separated by the threshold distance $R$.
5. Promote remaining isolated clusters as jets.

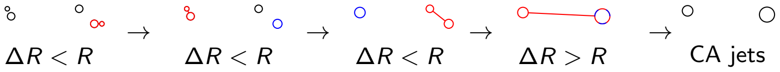

# Cambridge/Aachen Algorithm

Cambridge/Aachen Algorithm: a sequential clustering algorithm with a distance measure $(\Delta R)^2 = (\Delta\eta)^2 + (\Delta\phi)^2$

1. Check distances between objects.
2. Choose a pair of object having smallest $\Delta R$.
3. If the two object are separated by $\Delta R$ smaller than the threshold distance $R$, then merge the two objects in a shortest distance by summing their momenta.
4. Iterate above steps until every objects are separated by the threshold distance $R$.
5. Promote remaining isolated clusters as jets.

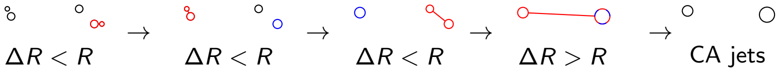


CA algorithm clusters objects in an order of increasing angle $\Delta R$. This clustering sequence can be understood as an imitation of parton branching, and hence it has an application to a jet substructure study.

# Mass drop tagger and filtering

Mass drop tagger utilize clustering sequence of CA algorithm

# Mass drop tagger and filtering

Mass drop tagger utilize clustering sequence of CA algorithm

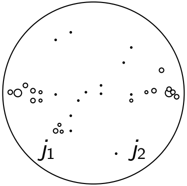

# Mass drop tagger and filtering

Mass drop tagger utilize clustering sequence of CA algorithm

1. Rewind clustering of a jet $j$. Label two subjets as $j_1$ and $j_2$ with $m_{j_1} > m_{j_2}$.

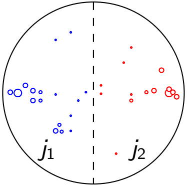

# Mass drop tagger and filtering

Mass drop tagger utilize clustering sequence of CA algorithm

1. Rewind clustering of a jet $j$. Label two subjets as $j_1$ and $j_2$ with $m_{j_1} > m_{j_2}$.
2. Mass drop can happen if rewinding clustering divides $j$ into subjets originated from light quarks.

$$m_{j_1} < \mu m_j \tag{10}$$

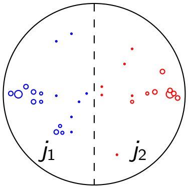

# Mass drop tagger and filtering

Mass drop tagger utilize clustering sequence of CA algorithm

1. Rewind clustering of a jet $j$. Label two subjets as $j_1$ and $j_2$ with $m_{j_1} > m_{j_2}$.
2. Mass drop can happen if rewinding clustering divides $j$ into subjets originated from light quarks.

$$m_{j_1} < \mu m_j \tag{10}$$

3. $p_T$ of jets are not too asymmetric

$$\frac{\min(p_{T,j_1}^2, p_{T,j_2}^2)}{m_j^2}(\Delta R_{j_1 j_2})^2 > y_{\rm cut} \tag{11}$$

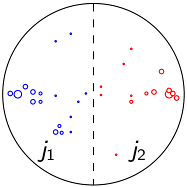

# Mass drop tagger and filtering

Mass drop tagger utilize clustering sequence of CA algorithm

1. Rewind clustering of a jet $j$. Label two subjets as $j_1$ and $j_2$ with $m_{j_1} > m_{j_2}$.
2. Mass drop can happen if rewinding clustering divides $j$ into subjets originated from light quarks.

$$m_{j_1} < \mu m_j \quad (10)$$

3. $p_T$ of jets are not too asymmetric

$$\frac{\min(p_{T,j_1}^2, p_{T,j_2}^2)}{m_j^2}(\Delta R_{j_1 j_2})^2 > y_{\rm cut} \quad (11)$$

4. If mass drop and $p_T$ asymmetry is not satisfied, repeat above procedure again for $j_1$.

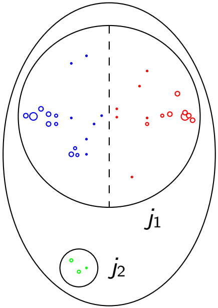

# Mass drop tagger and filtering

Mass drop tagger utilize clustering sequence of CA algorithm

1. Rewind clustering of a jet $j$. Label two subjets as $j_1$ and $j_2$ with $m_{j_1} > m_{j_2}$.
2. Mass drop can happen if rewinding clustering divides $j$ into subjets originated from light quarks.

$$m_{j_1} < \mu m_j \tag{10}$$

3. $p_T$ of jets are not too asymmetric

$$\frac{\min(p_{T,j_1}^2, p_{T,j_2}^2)}{m_j^2}(\Delta R_{j_1 j_2})^2 > y_{\rm cut} \tag{11}$$

4. If mass drop and $p_T$ asymmetry is not satisfied, repeat above procedure again for $j_1$.

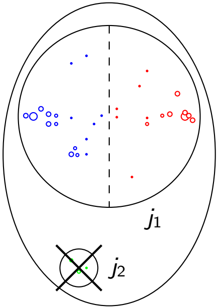

# Mass drop tagger and filtering

Mass drop tagger utilize clustering sequence of CA algorithm

1. Rewind clustering of a jet $j$. Label two subjets as $j_1$ and $j_2$ with $m_{j_1} > m_{j_2}$.
2. Mass drop can happen if rewinding clustering divides $j$ into subjets originated from light quarks.

$$m_{j_1} < \mu m_j \tag{10}$$

3. $p_T$ of jets are not too asymmetric

$$\frac{\min(p_{T,j_1}^2, p_{T,j_2}^2)}{m_j^2}(\Delta R_{j_1 j_2})^2 > y_{\mathrm{cut}} \tag{11}$$

4. If mass drop and $p_T$ asymmetry is not satisfied, repeat above procedure again for $j_1$.

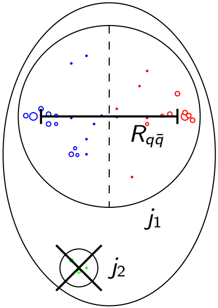


By finding mass-dropped clusters, we can find a relevant angular scale $R_{q\bar{q}}$ to resolve $Z \to q\bar{q}$.

# Mass drop tagger and filtering

Problem: Jets clustered with large angular scale is easily degraded by other QCD radiations.

$$m_q^2 = E_q^2 - |\vec{p}_q|^2 \ll E_q^2, |\vec{p}_q|^2 : \text{fine-tuned} \tag{12}$$

# Mass drop tagger and filtering

Problem: Jets clustered with large angular scale is easily degraded by other QCD radiations.

$$m_q^2 = E_q^2 - |\vec{p}_q|^2 \ll E_q^2, |\vec{p}_q|^2 : \text{fine-tuned} \tag{12}$$

Filtering:

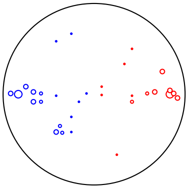

# Mass drop tagger and filtering

Problem: Jets clustered with large angular scale is easily degraded by other QCD radiations.

$$m_q^2 = E_q^2 - |\vec{p}_q|^2 \ll E_q^2, |\vec{p}_q|^2 : \text{fine-tuned} \tag{12}$$

Filtering:

1. Recluster jet constituent by more finer angular scale $R_{\text{filt}}$

$$R_{\text{filt}} = \min\left(0.3, \frac{R_{q\bar{q}}}{2}\right) \tag{13}$$

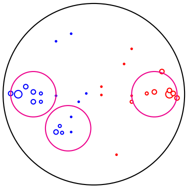

# Mass drop tagger and filtering

Problem: Jets clustered with large angular scale is easily degraded by other QCD radiations.

$$m_q^2 = E_q^2 - |\vec{p}_q|^2 \ll E_q^2, |\vec{p}_q|^2 : \text{fine-tuned} \tag{12}$$

Filtering:

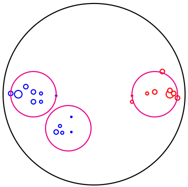

1. Recluster jet constituent by more finer angular scale $R_{\text{filt}}$

$$R_{\text{filt}} = \min\left(0.3, \frac{R_{q\bar{q}}}{2}\right) \tag{13}$$

2. Take $n_{\text{filt}}$ hardest subjets and discard others.

# Mass drop tagger and filtering

Problem: Jets clustered with large angular scale is easily degraded by other QCD radiations.

$$m_q^2 = E_q^2 - |\vec{p}_q|^2 \ll E_q^2, |\vec{p}_q|^2 : \text{fine-tuned} \tag{12}$$

Filtering:

1. Recluster jet constituent by more finer angular scale $R_{\text{filt}}$

$$R_{\text{filt}} = \min\left(0.3, \frac{R_{q\bar{q}}}{2}\right) \tag{13}$$

2. Take $n_{\text{filt}}$ hardest subjets and discard others.
3. $n_{\text{filt}} = 3$ is often chosen to catch an $\mathcal{O}(\alpha_S)$ radiation.

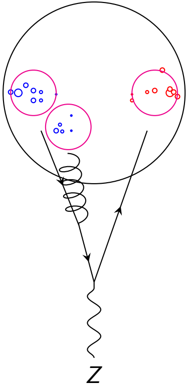

# Mass drop tagger and filtering

Problem: Jets clustered with large angular scale is easily degraded by other QCD radiations.

$$m_q^2 = E_q^2 - |\vec{p}_q|^2 \ll E_q^2, |\vec{p}_q|^2 : \text{fine-tuned} \quad (12)$$

Filtering:

1. Recluster jet constituent by more finer angular scale $R_{\text{filt}}$

$$R_{\text{filt}} = \min\left(0.3, \frac{R_{q\bar{q}}}{2}\right) \quad (13)$$

2. Take $n_{\text{filt}}$ hardest subjets and discard others.
3. $n_{\text{filt}} = 3$ is often chosen to catch an $\mathcal{O}(\alpha_S)$ radiation.

After then, we merged most soft filtered subjet into its nearest subjet in $\Delta R$.

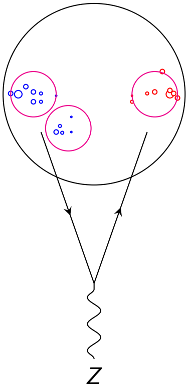

# Collimated Fermions from boosted $Z$ boson decay

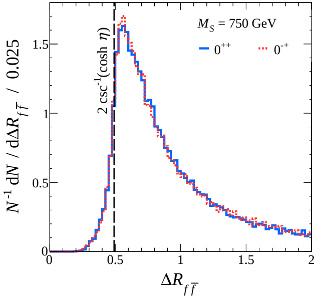


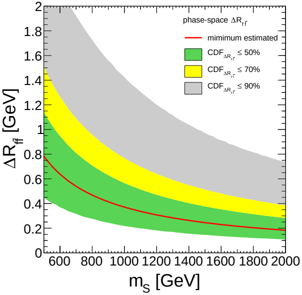

# Collimated Fermions from boosted $Z$ boson decay

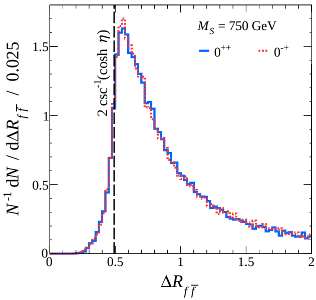


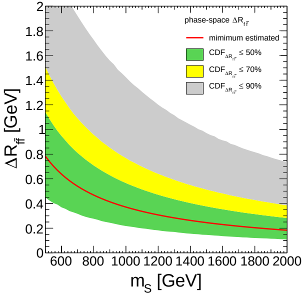


- As the mass gap between $S$ and $Z$ becomes larger, the angular separation of Fermions are getting smaller.

# Collimated Fermions from boosted $Z$ boson decay

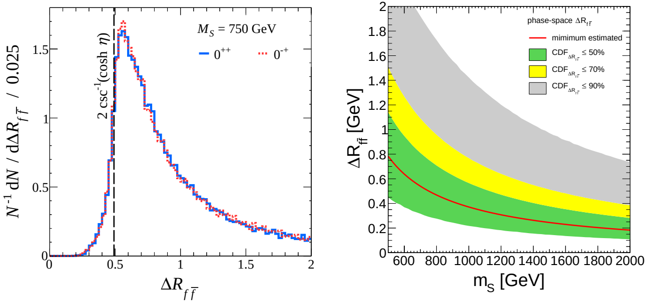


- As the mass gap between $S$ and $Z$ becomes larger, the angular separation of Fermions are getting smaller.
- For $m_S = 750\ \mathrm{GeV}$, intermediate region between resolved and collimated

$$\Delta R_{f\bar{f}} \gtrsim 0.5 \tag{14}$$

$$(\Delta R_{f\bar{f}})^2 = (\Delta\eta)^2 + (\Delta\phi)^2 \gtrsim \left(\frac{2m_Z}{p_{T,Z}}\right)^2 \tag{15}$$

# Collimated Fermions from boosted $Z$ boson decay

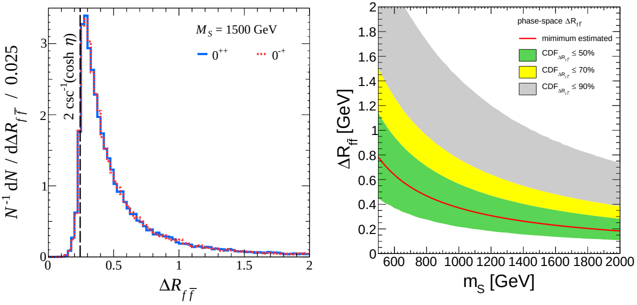


- As the mass gap between $S$ and $Z$ becomes larger, the angular separation of Fermions are getting smaller.
- For $m_S = 1500\ \mathrm{GeV}$, collimated

$$\Delta R_{f\bar{f}} \gtrsim 0.3 \tag{14}$$

$$(\Delta R_{f\bar{f}})^2 = (\Delta\eta)^2 + (\Delta\phi)^2 \gtrsim \left(\frac{2m_Z}{p_{T,Z}}\right)^2 \tag{15}$$

# Collimated Fermions from boosted $Z$ boson decay

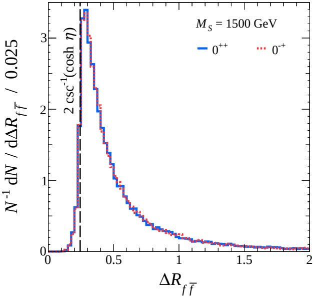


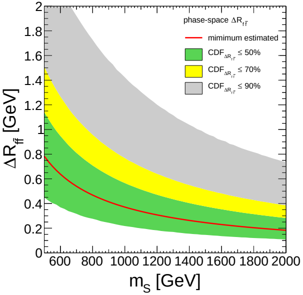


- As the mass gap between $S$ and $Z$ becomes larger, the angular separation of Fermions are getting smaller.
- Q: Is boosted object analysis effective for studying properties (such as spin and CP) of the resonance $S$?

# Collimated Fermions from boosted $Z$ boson decay

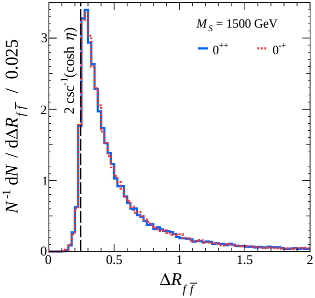


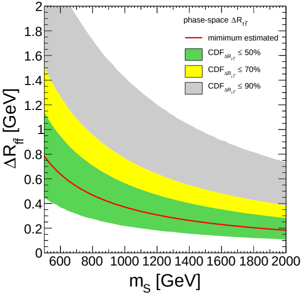


- As the mass gap between $S$ and $Z$ becomes larger, the angular separation of Fermions are getting smaller.
- Q: Is boosted object analysis effective for studying properties (such as spin and CP) of the resonance $S$?
- We will see that boosted object analysis is necessary in order to maximize the discrimination power for determining spin and CP of $S$.

# Angular separation of particles from $Z$ boson decay

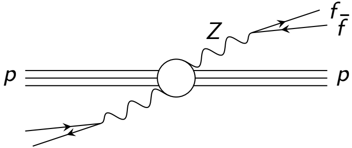


Lorentz invariant angular separtion under a boost along the beam direction

$$(\Delta R)^2 = (\Delta \eta)^2 + (\Delta \phi)^2 \approx \frac{m_Z^2}{p_{T,f}\, p_{T,\bar{f}}} \qquad (14)$$

# Angular separation of particles from $Z$ boson decay

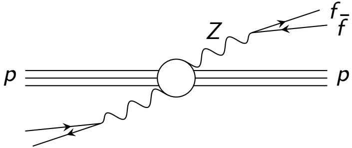


Lorentz invariant angular separtion under a boost along the beam direction

$$(\Delta R)^2 = (\Delta\eta)^2 + (\Delta\phi)^2 \approx \frac{m_Z^2}{p_{T,f}\,p_{T,\bar{f}}} \tag{14}$$

$\Delta R$ is from inner product between $p_f^\mu$ and $p_{\bar{f}}^\nu$. For massless $f$,

$$\eta_{\mu\nu} p_f^\mu p_{\bar{f}}^\nu = p_{T,f}\,p_{T,\bar{f}}(\cosh\Delta\eta - \cos\Delta\phi) \tag{15}$$

$$\cosh\Delta\eta - \cos\Delta\phi = \frac{\eta_{\mu\nu} p_f^\mu p_{\bar{f}}^\nu}{p_{T,f}\,p_{T,\bar{f}}} = \frac{m_Z^2}{2p_{T,f}\,p_{T,\bar{f}}} \tag{16}$$

# Angular separation of particles from $Z$ boson decay

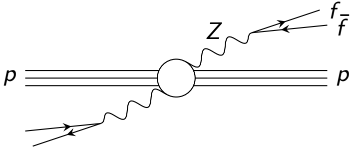


Lorentz invariant angular separtion under a boost along the beam direction

$$(\Delta R)^2 = (\Delta\eta)^2 + (\Delta\phi)^2 \approx \frac{m_Z^2}{p_{T,f}\, p_{T,\bar{f}}} \tag{14}$$

$\Delta R$ is from inner product between $p_f^\mu$ and $p_{\bar{f}}^\nu$. For massless $f$,

$$\eta_{\mu\nu} p_f^\mu p_{\bar{f}}^\nu = p_{T,f}\, p_{T,\bar{f}} (\cosh\Delta\eta - \cos\Delta\phi) \tag{15}$$

$$\cosh\Delta\eta - \cos\Delta\phi = \frac{\eta_{\mu\nu} p_f^\mu p_{\bar{f}}^\nu}{p_{T,f}\, p_{T,\bar{f}}} = \frac{m_Z^2}{2 p_{T,f}\, p_{T,\bar{f}}} \tag{16}$$

In terms of $p_{T,Z}$ we can rewrite $\Delta R$ by

$$(\Delta R)^2 = (\Delta\eta)^2 + (\Delta\phi)^2 \approx \frac{1}{z(1-z)} \frac{m_Z^2}{p_{T,Z}^2}, \quad z(1-z) = \frac{p_{T,f}\, p_{T,\bar{f}}}{p_{T,Z}^2} \tag{17}$$

$$(\Delta R)^2 \approx \frac{1}{z(1-z)} \frac{m_Z^2}{p_{T,Z}^2} \geq \left(\frac{2m_Z}{p_{T,Z}}\right)^2 \qquad (18)$$

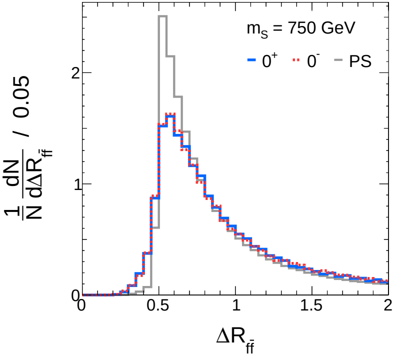


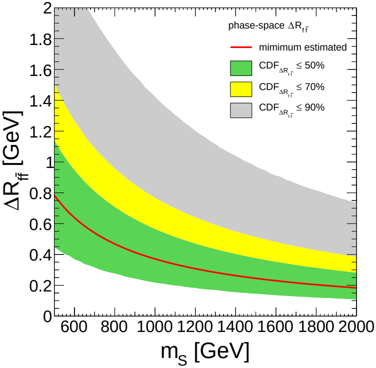


For $m_S = 750\ \mathrm{GeV}$ resonance, $\Delta R \gtrsim 0.5$. For electron (jet) isolation in reconstruction level, we often set an isolation angular scale 0.3 (0.4).